

Effect of Grid Size on the Computation of Free-Surface Waves

Seung-Hyun Kwag*

(96년 11월 14일 접수)

자유표면과 계산에서의 격자크기영향

곽 승 현*

Key Words : Grid Size(격자크기), Free-Surface Waves(자유표면파), Viscous Flows(점성유동), Multi-Grid(복합격자), Triple Mesh Method(3중격자법)

초 록

수치격자의 크기제한에 의한 자유표면 유동해석 문제를 효율적으로 다루기 위하여 자유표면의 모든 격자를 x 방향으로 4, 8, 12개로 등분할하고, y 방향으로는 4개로 잘게 잘라서 계산하였다. 이중격자 또는 삼중격자로 Navier-Stokes 방정식의 각항에 크기가 다른 격자를 사용해 효율을 향상시키는 계산방법의 연장으로, 본 논문에서는 자유표면 방정식에 보다 세분화된 격자를 적용해, Marker Particle 이동 및 자유수면형성에 효율향상을 줄수 있는 수치방법을 도입하였다. 계산결과에 의하면 초기사용 격자가 coarse한 경우가 본방법의 효과가 커짐을 알수 있고 대상물체로는 층류유동에서 Wigley모형과 난류유동의 S103 모형이다.

1. INTRODUCTION

To overcome the deficiency of computer's hardware, many numerical techniques have been developed by the finite difference method. But the method still faces a serious problem because it requires very long CPU time and a huge memory storage for accurate simulation. Recently, the improvement of the efficiency has been strongly

demand. The method of IAF, a kind of implicit scheme, the method of local time step, etc. are the examples for more efficient computations. Some comparative calculations by these methods have been carried out. It seems that IAF⁽¹⁾ is quite promising to speed up the calculation but its formulation is a little complicated. For the numerical truncation error to be small enough to have little effect on the physical performance, the

* 한라공과대학교 조선공학과

mesh size should be strictly considered. The mesh size must be extremely small for high Reynolds-number flows to meet this demand. However, such fine meshes are not always necessary for all the equations and terms. For example, the truncation errors of the Poisson equation for the pressure of the non-convective terms in Navier-Stokes equation do not have much influence on the results as the convection terms do. The hybrid type of the mesh may make the computations more efficient. One possibility is to employ different mesh systems depending on the characteristics of the equations or the terms. We call such a method "double mesh method"⁽²⁾ or "triple mesh method"⁽³⁾, written in short as DMM or TMM hereafter. It was first proposed for numerical simulations of 3-D nonlinear free-surface flow problems by boundary element method⁽⁴⁾. In order to reduce the numerical viscosity as much as possible, a very fine mesh system which contains about 60 grids⁽⁵⁾ in one wave length is used in the finite difference calculation concerned with the free-surface equations, while the governing Laplace equation is solved on a relatively coarse mesh system which contains about 10 grids in one wave length by the boundary element method. The computed results by DMM or TMM were of enough accuracy and both the computing time and the size of the memory storage were remarkably reduced.

In the present paper, a multi-grid on the free-surface is introduced in the finite difference solver of the Navier-Stokes equation to improve the calculation efficiency. As mentioned above, the demands to the mesh size are not the same for all the equations and the terms in the finite difference method. So it is expected that some improvement, similar to that achieved in the simulation of free-surface problem by DMM or TMM, may be made by introducing more fine meshes in the conventional finite difference method.

2. NUMERICAL STRATEGY

A single grid system⁽⁶⁾ is usually used in the whole computation whose minimum size is determined for the numerical diffusion to be less than that by viscosity. The grid size for the calculation of the free-surface elevation must be determined by a different scale, the minimum wave length. In the simulation, two or three mesh systems are usually used whose sizes are different each other depending on the characteristic of equations. The first one is for the convective terms in the Navier-Stokes equation, the second one is for the Poisson equation, and the third one is for the free-surface equation. The third grid system requires the finest mesh. In the present calculation, the third one is numerically confirmed; more fine grids are used to improve the accuracy of free-surface calculation with relatively less computer storage. One element of the free-surface is discretized into $(4x_{ii}, 4x_{jj})$, $(8x_{ii}, 4x_{jj})$, $(12x_{ii}, 4x_{jj})$ fine grids because the free-surface waves are much affected by the grid size in the finite-difference scheme. Fig.1 shows the shape of $(4x_{ii}, 4x_{jj})$ discretization.

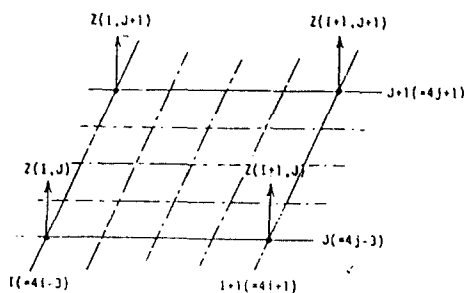


Fig. 1 Discretization of grid on free-surface($4x_{ii}, 4x_{jj}$ case)

The positions, or Lagrangian coordinates, of each particle (x_p^n, y_p^n, z_p^n) are obtained by numerical integration from some initial position (x_p^0, y_p^0, z_p^0) at

time $t=0$;

$$\begin{aligned} x_p^n &= x_p^0 + \int^t u_p \cdot dt \\ y_p^n &= y_p^0 + \int^t v_p \cdot dt \\ z_p^n &= z_p^0 + \int^t w_p \cdot dt \end{aligned} \quad (1)$$

where u_p, v_p, w_p are the velocities in the Eulerian mesh at the time dependent location of the particle. In the present MAC-based codes, the particle velocities are evaluated by two-variable linear interpolation. Consistently with the forward time integration of MAC method, (1) is evaluated sequentially as (2).

$$\begin{aligned} x_i^{n+1} &= x_i^n + u_i^n \cdot \Delta t \\ y_i^{n+1} &= y_i^n + v_i^n \cdot \Delta t \\ z_i^{n+1} &= z_i^n + w_i^n \cdot \Delta t \end{aligned} \quad (2)$$

(2) is the Lagrangean expression of the kinematic condition on the free-surface. The condition can also be expressed in the Euler form as follows;

$$\partial \zeta / \partial t = -u \cdot \partial \zeta / \partial x - v \cdot \partial \zeta / \partial y + w \quad (3)$$

where ζ and t are the free-surface elevation and the time respectively. Numerically (2) is equivalent to (3) if the 1st order upstream difference scheme is used in (3).

The shape of the free-surface is not known a priori; it is defined by the position of the marker particles. We note here that the boundary conditions at the free-surface require zero tangential stress and a normal stress which balances any externally applied normal stress. The application of these conditions requires a knowledge of not only the location of the free-surface at each grid but also its slope and curvature. In our calculation, the z -coordinate of the free surface is re-arranged by the bivariate linear interpolation in proportion to the newly calculated projected area at each time-step. The details on the free-surface are described in the appendix.

3. COMPUTATION AND DISCUSSION

3.1 Wigley Case in Laminar Flows

In order to check the convergence of the results, the wave patterns at $T=2.5$ and 3.0 are compared at $Fr=0.316$ and $Re=10^4$ where T is the nondimensional time. It is originated from the previous result⁽⁷⁾. To review the effects of more fine grids adopted on the free surface, four kinds of grids are applied to the computation. The size of regular grid is $104 \times 29 \times 19$ (here $ii=104, jj=29$ on free surface). Fig.2 shows the wave patterns obtained by the regular grid. Fig.3 uses the grid of $(4xii, 4xjj)$ on free surface and gives us about 10% improvement in the free surface development, compared with those by regular grid. It means that the size of grid is very important in developing the marker particles on free surface. Fig.4 and Fig.5 use that of $(8xii, 4xjj)$ on free surface. They show the improvement of about 16% at $T=2.5$ and 17% at $T=3.0$, respectively. However, the change is hardly seen in the free-surface patterns after $t=3.0$. There seems to be some limitations in the scheme of finite difference method for the free-surface generation. Fig.6 uses that of $(12xii, 4xjj)$ on free surface. Some more improvement can be obtained; 21.4% compared with that of regular grid at $T=3.0$.

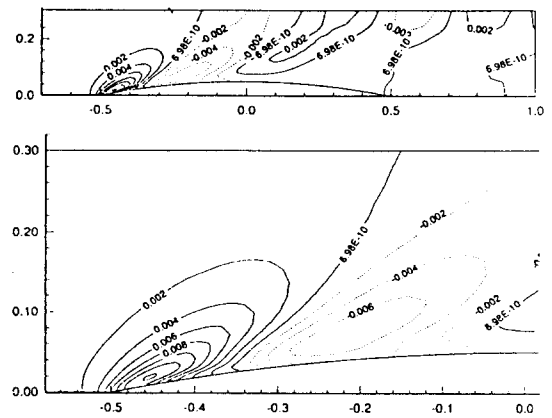


Fig. 2 Free-surface contour by regular grid(ii, jj) for wigley case

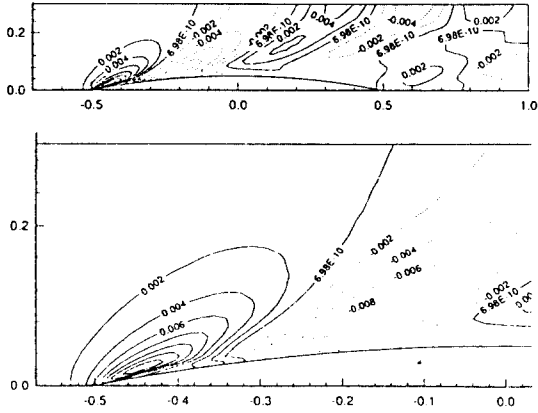


Fig. 3 Free-surface contour by multi-grid(4xii, 4xjj) for wigley case

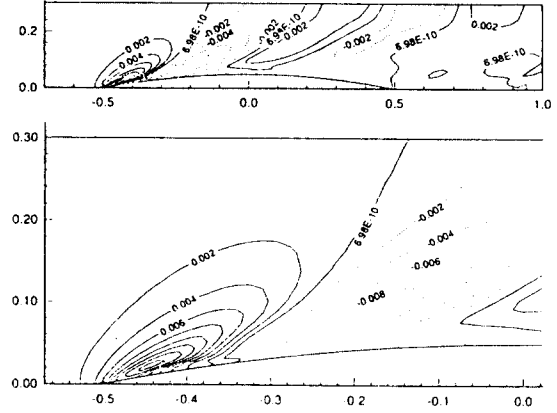


Fig. 6 Free-surface contour by multi-grid(12xii, 4xjj) for wigley case

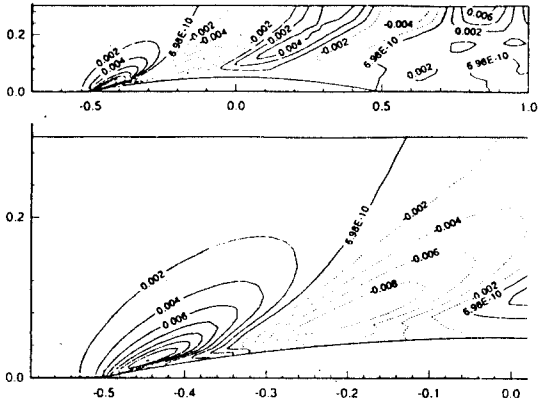


Fig. 4 Free-surface contour by multi-grid(8xii, 4xjj) at t=2.5 for wigley case

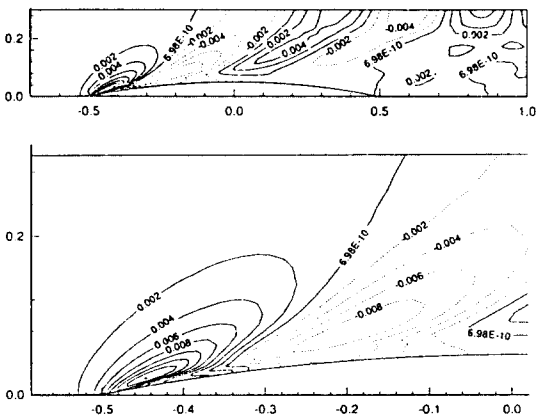


Fig. 5 Free-surface contour by multi-grid(8xii, 4xjj) at t=3.0 for wigley case

3.2 S-103 Case in Turbulent Flows

To confirm the numerical efficiency of the multi grid, the high Reynolds-number free surface wave of S-103 is also studied. S-103 is an Inuid model with the beam/length ratio of 0.09. In the present case, calculations are made at $R_n=10^6$ and $F_n=0.28$ with Baldwin-Lomax turbulence model. The result is that at the time $T=3.0$, when the convergence is well assured. The grid size of regular type is $74 \times 29 \times 30$ and the multi-grid on the free-surface is numerically tried. Fig.7 shows the wave patterns obtained by the regular grid. Fig.8 uses the grid of (4xii,4xjj) on free surface and gives us about 7% improvement in the free-surface development, compared with that by regular grid. It means that the size of grid is very important in moving the marker particles on free surface. Fig.9 uses that of (8xii,4xjj) on free-surface. It shows the improvement of about 19% at $T=3.0$. Fig.10 uses that of (12xii,4xjj) on free-surface. Some more improvement is obtained; 29% compared with that of regular grid at $T=3.0$.

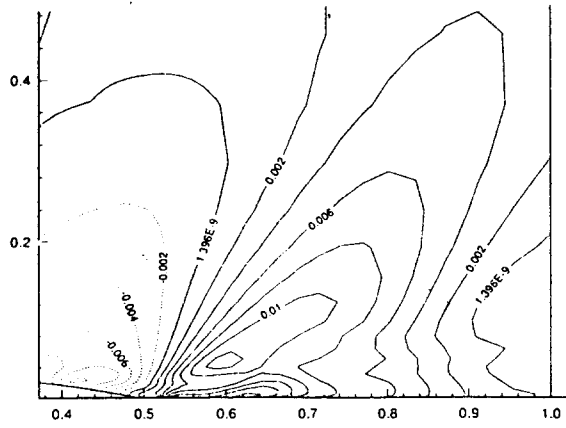
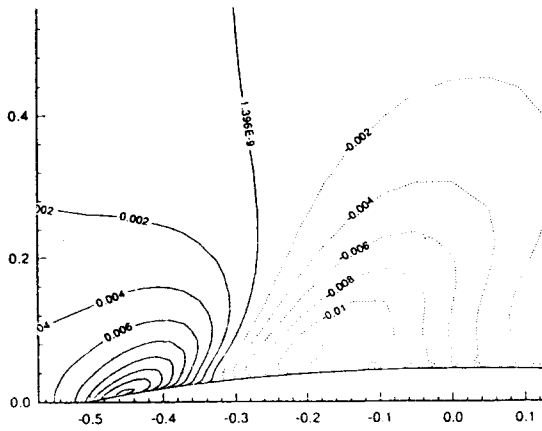


Fig. 7 Free-surface contour by regular grid (ii, jj) for S103 case

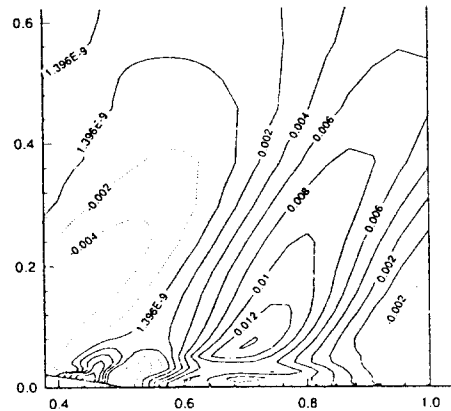
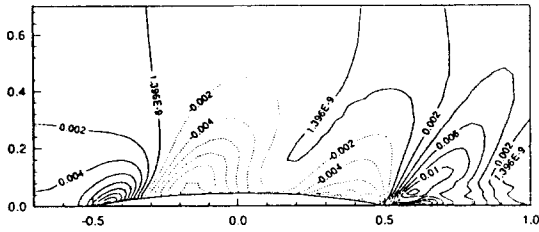
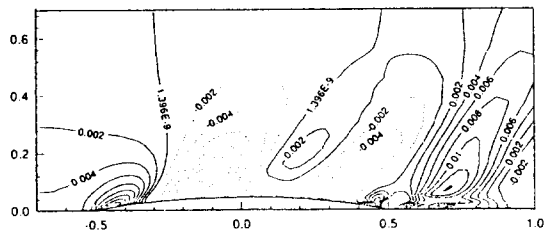
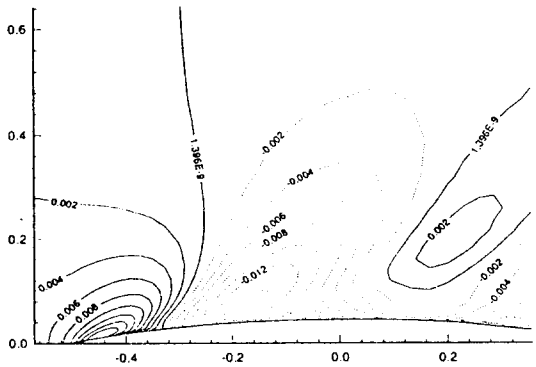


Fig. 8 Free-surface contour by multi-grid (4xii, 4xjj) for S103 case



Effect of Grid Size on the Computation of Free-Surface Waves

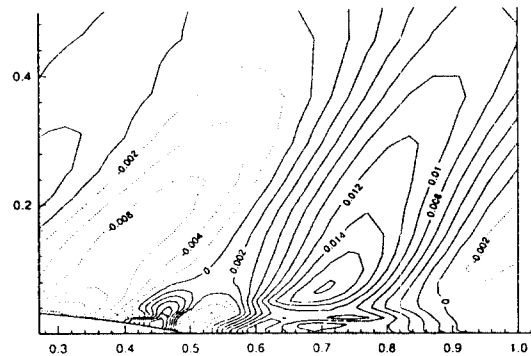
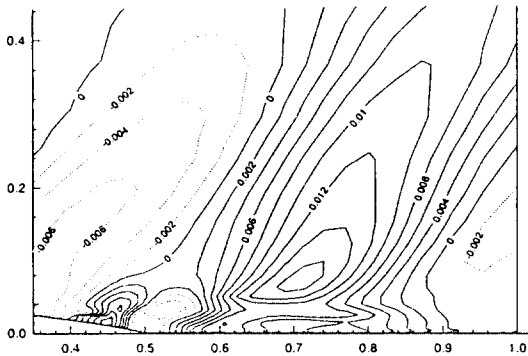
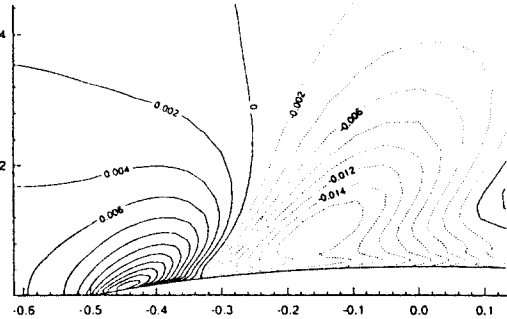
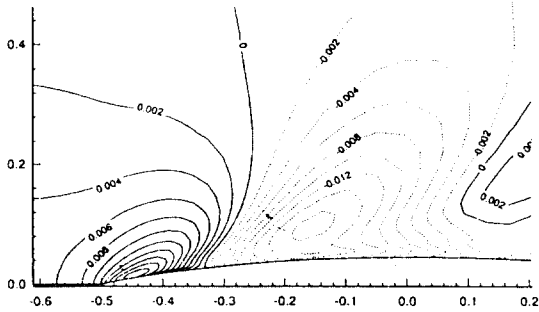
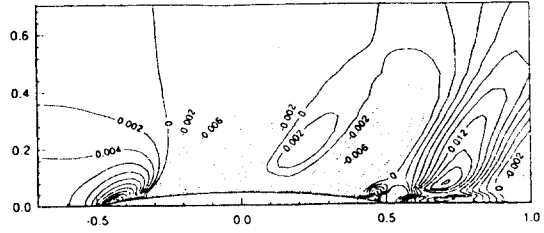
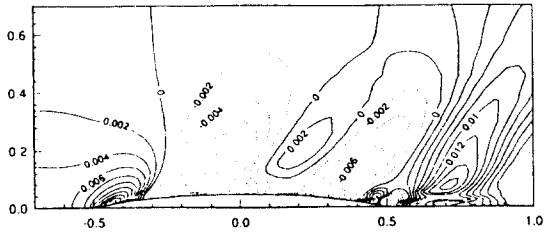


Fig. 9 Free-surface contour by multi-grid (8xii, 4xjj) for S103 case

Fig. 10 Free-surface contour by multi-grid (12xii, 4xjj) for S103 case

4. CONCLUSION

In order to calculate the free surface wave efficiently, the multi-grid method is applied for the finite difference solution of Navier-Stokes equation. The method is to use the multi grid system on the free surface. Through several comparative computations, it is found that the method is significantly effective for the free surface calculation.

5. REFERENCES

- 1) Kodama, Y., "Computation of High Reynolds Number Flows past a Ship Hull Using the IAF Scheme", Jour of Soc of Naval Arch of Japan, Vol.161, 1987
- 2) Xu, Q., Mori, K., Shin, M., "Double Mesh Method for Efficient Finite Difference Calculation", Jour of Soc of Naval Arch of Japan, Vol.166, 1989

- 3) Mori,K., Kwag,S., Doi,Y., "Numerical Simulation of Ship Wave and Some Discussions on Bow Wave Breaking and Viscous Interaction of Stern Wave", 18th Symp on Naval Hydrodynamics, U.S.A.,1990
- 4) Xu,Q, Mori,K, "Numerical Simulation of 3-D Nonlinear Water Wave by Boundary Element Method", Jour of Soc of Naval Arch of Japan, Vol.165,1989
- 5) Shin,M, Mori,K, "Numerical Computation of 2-D Waves behind a Hydrofoil", Jour of Soc of Naval Arch of Japan, Vol.163,1988
- 6) Hino,T., "Numerical Computation of a Free Surface Flow around a Submerged Hydrofoil by the Euler/Navier-Stokes Equations", Jour of Soc of Naval Arch of Japan, Vol.164,1988
- 7) Kwag,S.H., Mori,K., Shin,M., "Numerical Computation of 3-D Free Surface Flows by N-S Solver and Detection of Sub-Breaking", Jour of Soc of Naval Arch of Japan, Vol.166,1989
- 8) Mori,K., Kwag,S.H., Doi,Y., "Numerical Simulation of Ship Waves and Some Discussions on Bow Wave Breaking & Viscous Interaction of Stern Waves", 18th Symp on Naval Hydro.,USA, 1990

respectively. In the present research, the x, y coordinates of the grids on the free surface are fixed and z coordinate moves freely. The elevation of the new free surface grid Q_i can be determined by P'_{i-1} and P'_i as follows:

$$\xi_i^{n+1} = z_i' + k \cdot (X_i - X_{i-1}') \quad (A1)$$

where

$$k = (Z_i' - Z_{i-1}') / (X_i' - X_{i-1}') \quad (A2)$$

$$= \{ Z_i^n - Z_{i-1}^n + (w_i^n - w_{i-1}^n) \cdot \Delta t \} / \{ x_i - x_{i-1} + (u_i^n - u_{i-1}^n) \cdot \Delta t \}$$

ξ_i^{n+1} can be further expressed as

$$\xi_i^{n+1} = \xi_i^n + w_i^n \cdot \Delta t - (u_i^n \Delta t) \cdot (\xi_i^n - \xi_{i-1}^n) / (x_i - x_{i-1}) \cdot \{ 1 + (\Delta w / \Delta x) \Delta t \} / \{ 1 + (\Delta u / \Delta x) \Delta t \} \quad (A3)$$

or

$$(\xi_i^{n+1} - \xi_i^n) / \Delta t = w_i^n - u_i^n \cdot (\xi_i^n - \xi_{i-1}^n) / \Delta x \cdot \{ 1 + (\Delta w / \Delta x) \Delta t \} / \{ 1 + (\Delta u / \Delta x) \Delta t \} \quad (A4)$$

where

$$\Delta w / \Delta x = (w_i^n - w_{i-1}^n) / (x_i - x_{i-1}) \quad (A5)$$

$$\Delta u / \Delta x = (u_i^n - u_{i-1}^n) / (x_i - x_{i-1})$$

Appendix : Lagrangian Expression of Kinematic Free Surface Condition

Suppose $P_{i-1}(X_{i-1}, Z_{i-1}^n)$ and $P_i(X_i, Z_i^n)$ are two grids on the free surface at $t=n$ as shown in Fig.11. At the next time step $t=n+1$, these mark points move to $P'_{i-1}(X'_{i-1}, Z'_{i-1})$ and $P'_i(X'_i, Z'_i)$

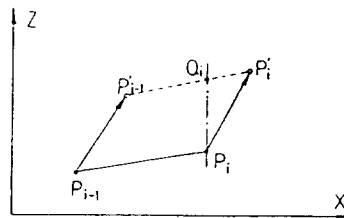


Fig. 11 Coordinate for free-surface movement